Phonon Resonances Associated with Interstitial Atoms in Germanium and Silicon*

DAVID K. BRICE
Sandia Laboratory, Albuquerque, New Mexico
(Received 21 June 1965)

The resonant scattering of acoustic phonons by interstitial atoms at the $(\frac{1}{2},\frac{1}{2},\frac{1}{2})$ position in the Si and Ge lattices has been investigated using the Green's-function matrix technique of Lifshitz. The lattice contribution to the Green's function is calculated using a spherically symmetric phonon spectrum with transverse and longitudinally polarized phonons. The observed dispersion relation along the (1,0,0) direction is included in the calculation. The interstitial contribution to the Green's function is calculated exactly and dominates at low frequencies. The interaction matrix is constructed from nearest- and next-nearest-neighbor interactions and limited in form by symmetry considerations. The interaction matrix and interstitial mass M are the independent variables in the calculation. The resonance frequency ω and width $\Delta\omega$ are calculated as functions of the force constants of the interaction matrix and interstitial mass. Results show that a single effective force constant K can be defined such that $\omega \propto (K/M)^{1/2}$ and $\Delta\omega/\omega \propto \omega^3 M$ over most of the transverse acoustic band. Thus, a measurement of both quantities ω and $\Delta\omega$ should allow an unambiguous determination of K and M. Several methods are proposed for observing interstitial resonances.

I. INTRODUCTION

THE internal motions of crystals may be described as composed of the superposition of a number of traveling-wave modes or phonons which are characteristic of the crystal. Many of the measurable properties of the crystal are derivable from a knowledge of these modes, their interactions with each other, and their interactions with external radiations. Likewise, many of the properties of the phonon field may be inferred from measurements of crystal properties. A good example is the construction of phonon dispersion relations from inelastic scattering of thermal neutrons.[1]

When defects are present in the lattice, the phonon spectrum is altered and so in turn are the crystal properties which are dependent on the phonons. Observation of the frequency and response shape of phonon-scattering resonances associated with such defects should provide a method for determining some of the properties of the interactions of interest. In the neighborhood of a defect exhibiting a phonon resonance, large amplitudes of vibration will build up at the resonance frequency and interactions between the phonon field and other processes which occur in the vicinity of the defect should be observed. For example, an increase in spin-lattice interaction strength, enhanced phonon-assisted electronic transitions, and increased infrared absorption for charge-associated defects would be expected.

The general theory for handling such defects has been developed by Lifshitz,[2] Koster and Slater,[3] and Lax.[4] Techniques for calculating the various thermodynamic functions have been developed by Lifshitz,[2] Montroll and Potts,[5] and Mahanty, Maradudin, and Weiss.[6] The method of double-time Green's functions has also been applied to the theory by Elliott and Taylor.[7] Applications of the theory to resonant scattering have been considered in general by Klein,[8] Takeno,[9] Krumhansl,[10] and Elliott and Taylor.[7] Specific applications have considered vacancies[10,11] and substitutional mass defects.[7–10,12–15] Recently, Wagner[15] considered resonant scattering of phonons by the internal modes of molecules substituted into the lattice. The interstitial has been considered only in the linear chain by Montroll and Potts.[5]

The resonant scattering of phonons by vacancies or interstitials has not been treated for diamond-type lattices even though the properties of such defects are of great interest in studies of radiation damage in silicon and germanium. Vacancy production in these covalent materials, however, is accompanied by a reformation of the broken atomic bonds in such a manner as to appreciably reduce the local symmetry.[16] An analysis of this low-symmetry, strongly bonded defect would

* This work was supported by the U. S. Atomic Energy Commission.

[1] B. N. Brockhouse and P. K. Iyengar, Phys. Rev. **111**, 747 (1958); B. N. Brockhouse, Phys. Rev. Letters **2**, 257 (1959) and others. See also, *Inelastic Scattering of Neutrons in Liquids and Solids* (International Atomic Energy Agency, Vienna, 1961, 1962), Vols. I and II.

[2] I. M. Lifshitz, Nuovo Cimento Suppl. **3**, 733 (1956), and references in this paper.

[3] G. F. Koster and J. C. Slater, Phys. Rev. **94**, 1392 (1954); **95**, 1167 (1954).

[4] M. Lax, Phys. Rev. **94**, 1391 (1954).

[5] E. W. Montroll and R. B. Potts, Phys. Rev. **100**, 525 (1955); **102**, 72 (1956).

[6] J. Mahanty, A. A. Maradudin, and G. Weiss, Progr. Theoret. Phys. (Kyoto) **24**, 1055 (1960).

[7] R. J. Elliott and D. W. Taylor, Proc. Phys. Soc. (London) **83**, 189 (1964).

[8] M. V. Klein, Phys. Rev. **131**, 1500 (1963).

[9] S. Takeno, Progr. Theoret. Phys. (Kyoto) **29**, 191 (1963).

[10] J. A. Krumhansl, Report of the Copenhagen Conference on Lattice Dynamics, 1963 (unpublished).

[11] G. F. Nardelli and N. Terzi, J. Phys. Chem. Solids **25**, 815 (1964).

[12] R. Brout and W. Visscher, Phys. Rev. Letters **9**, 54 (1962).

[13] P. G. Dawber and R. J. Elliott, Proc. Roy. Soc. (London) **A273**, 222 (1963); Proc. Phys. Soc. (London) **81**, 453 (1963).

[14] G. W. Lehmann and R. E. DeWames, Phys. Rev. **131**, 1008 (1963).

[15] M. Wagner, Phys. Rev. **131**, 1443 (1963).

[16] R. A. Swalin, J. Phys. Chem. Solids **18**, 290 (1961); G. D. Watkins, J. Phys. Soc. Japan **18**, 22 (1962).

yield a quite complicated dependence of resonance properties on the variable-interaction matrix. It is doubtful that a comparison of the results of such an analysis with experiment would yield much information regarding the actual properties of the vacancy because of the complexity of this dependence. The interstitial, on the other hand, is relatively weakly bound[17] and should not disturb the local symmetry appreciably if it is located on a single atomic site, as assumed in the present paper. The resultant analysis should then be less complicated than that for the vacancy.

In this paper the resonance scattering of phonons by interstitial atoms in the Ge and Si lattices is examined by the Green's-function technique of Lifshitz.[2] The interstitials are considered to occupy the $(\frac{1}{2},\frac{1}{2},\frac{1}{2})$ position in the unit cell, and the resonance frequency and width are calculated for various values of the force constants and interstitial mass.

The Green's-function matrix method is outlined briefly in Sec. II and applied to the interstitial problem. In Sec. III the symmetry properties of the interstitial environment are exploited to simplify the problem, and a description of the numerical calculations is contained in Sec. IV. The results of the calculations are presented and discussed in Sec. V, and the conclusions and summary are contained in Sec. VI.

II. THE GREEN'S-FUNCTION MATRIX METHOD

A. General Theory

The Green's-function technique of Lifshitz[2] offers a particularly straightforward method of treating the vibrational spectrum of a perturbed crystal by reducing the problem to a small number of dimensions, compatible with the complexity of the perturbation. The method has been discussed and applied frequently in the literature,[2,8,11–15] but it is reproduced here in abbreviated form for clarity and as an introduction to the notation of the following sections.

The internal dynamics of an unperturbed crystal composed of N atoms are described in the harmonic approximation by the eigenvectors v_{kp} and the eigenvalues ω_{kp}^2 of the characteristic matrix D, of the crystal through[18]

$$(D-\omega_{kp}^2 I)v_{kp}=0. \tag{1}$$

The v_{kp} represent the normal modes, or phonons, of the crystal with ω_{kp} being the corresponding vibrational frequency. In an infinite crystal the subscript $\mathbf{k}$ is the propagation vector of the phonon. In a finite crystal the identification of $\mathbf{k}$ with the propagation vector will be valid for $k\gg 2\pi/a$, where a is the dimension of the crystal (i.e., the identification is valid for phonons with wavelength much smaller than the crystal dimensions). The subscript p is a polarization index and serves to distinguish between phonons having the same $\mathbf{k}$.

The $3N\times 3N$ matrix D is related to the crystal potential energy V through

$$D_{ij}=(M_iM_j)^{-1/2}(\partial^2 V/\partial u_i\partial u_j)\equiv(M_iM_j)^{-1/2}V_{ij}. \tag{2}$$

The $3N$ coordinates u_i represent the set of Cartesian displacements of the atoms from their equilibrium positions. The mass M_i is the mass of the atom to which the coordinate u_i refers. Since three of the u_i will refer to the same atom, the corresponding three M_i must necessarily be equal.

In general with the introduction of a defect which changes both the crystal potential and some of the atomic masses, the internal dynamics of the perturbed crystal are described by the solutions v and ω^2 of the equation

$$(D-\omega^2 I+\Gamma)v=0. \tag{3}$$

The perturbation matrix Γ is given by

$$\Gamma_{ij}=[\Delta V_{ij}/(M_iM_j)^{1/2}]-\omega^2(\Delta M_i/M_i)\delta_{ij}, \tag{4}$$

where ΔV_{ij}, the change in V_{ij}, and ΔM_i, the change in M_i, characterize the perturbation, and δ_{ij} is the Kronecker delta.

The effect of the perturbation on the crystal dynamics may be given at least two distinct, but equivalent, interpretations. First, Eq. (3) may be viewed as a scattering problem. In this case it is appropriate to calculate a scattering matrix and look for resonances in the scattering. Alternatively, Eq. (3) may be viewed as an eigenvalue problem, similar to Eq. (1), but with changed values for some of the elements of D. In this case the appropriate solutions to (3) are a new set of frequencies and normal modes. Correspondence may be made between the two descriptions by noting that the resonance scattering in the first description corresponds in the second description to normal modes at the same frequency having larger amplitudes of vibration in the vicinity of the defect than at other locations in the crystal.

The scattering problem may be solved by introducing the Green's-function matrix G defined as a solution to

$$G(\omega^2)[D-\omega^2 I]=I. \tag{5}$$

Solutions to (5) exist for ω^2 not an eigenvalue of D. Choosing $\omega^2=\omega^2{}_{kp}+i|\epsilon|$ gives the outgoing scattered-wave Green's function.[8] After calculation of the scattering matrix the parameter $|\epsilon|$ may be allowed to go to zero. An explicit representation of $G(\omega^2)$ is given by

$$G(\omega^2)=\sum_{k,p}\frac{v_{kp}v_{kp}^{\dagger}}{\omega^2{}_{kp}-\omega^2}, \tag{6}$$

where the v_{kp} and ω_{kp}^2 are solutions to (1), and $v_{kp}^{\dagger}$ is the Hermitian transpose of v_{kp}.

The scattering solutions to (3) are divided into an incident part v_{kp} and a scattered part w_{kp}; then with the

[17] K. H. Bennemann, Phys. Rev. **137**, A1497 (1965).

[18] The symbol k appearing as a subscript or summation index will mean the vector $\mathbf{k}$ unless otherwise indicated.

help of (1), (3), and (5) it can be shown that

$$w_{kp}=-G\Gamma(1+G\Gamma)^{-1}v_{kp}. \tag{7}$$

With T defined by

$$T=\Gamma(1+G\Gamma)^{-1}, \tag{8}$$

Eq. (7) becomes

$$w_{kp}=-GTv_{kp}. \tag{9}$$

Normally, Γ will be nonzero only in a small subspace of the $3N$-dimensional space of the crystal. It follows from (8) that T is nonzero only in the same subspace.[19] If g, t, and γ represent the projection of G, T, and Γ onto the nonzero subspace of Γ, then an explicit representation for t is

$$t=\sum_s \frac{\gamma\xi_s\eta_s}{1+\lambda_s}, \tag{10}$$

where η_s is the left eigenvector of the matrix $g\gamma$ belonging to the eigenvalue λ_s, and ξ_s is the corresponding right eigenvector. Since $g\gamma$ is not necessarily a Hermitian matrix, η_s may not be the Hermitian transpose of ξ_s.

The projection of w_{kp} onto the nonzero subspace of Γ, Pw_{kp}, is given by

$$Pw_{kp}=-\sum_s \frac{\lambda_s\xi_s(\eta_s,v_{kp})}{1+\lambda_s}, \tag{11}$$

from which the resonance condition

$$\left|\frac{\lambda_r(\omega_r)}{1+\lambda_r(\omega_r)}\right|=\text{maximum}, \tag{12}$$

with ω_r as resonance frequency, is obtained. For sharp resonances, the full width at half-maximum will then be given by

$$\Delta\omega=2|\omega_{1/2}-\omega_r|=\left|\frac{\mathrm{Im}\lambda_r(\omega_r)}{(d\,\mathrm{Re}\lambda_r/d\omega)_{\omega=\omega_r}}\right|. \tag{13}$$

The problem of locating resonances associated with the perturbation then reduces to one of evaluating and diagonalizing $g\gamma$ over the range of frequencies of interest. The resonance width may be determined from (13), or directly from (12).

The scattering amplitude will depend on the matrix elements

$$(v_{k'p'},w_{kp})=-\sum_s \frac{(v_{k'p'},G\gamma\xi_s)(\eta_s,v_{kp})}{1+\lambda_s}. \tag{14}$$

From (14) it is seen that the coupling of a particular phonon into the resonance depends on the left eigenvectors η_s through (η_s,v_{kp}), while the coupling of a particular phonon out of the resonance depends on the right eigenvectors ξ_s through $(v_{kp},G\gamma\xi_s)$.

[19] To obtain this result expand the operator $(1+G\Gamma)^{-1}$ in a Taylor series. Each term of $\Gamma(1+G\Gamma)^{-1}$ is then of the form $\Gamma(G\Gamma)^n$ which has the desired property. See also Ref. 8.

B. Application to the Interstitial

The theory of Sec. IIA is applied to the interstitial problem by including the interstitial in the unperturbed lattice, but with infinitesimal coupling. Three of the solutions to (1) are then the three Cartesian coordinates of the interstitial, (u_1,u_2,u_3), with corresponding $\omega^2=0$. The remaining solutions are the usual traveling-wave phonons of the perfect lattice. The Green's function then becomes, using (6),

$$G(\omega^2)=\sum_{\text{Phonons}} \frac{v_{kp}v_{kp}^{\dagger}}{\omega^2{}_{kp}-\omega^2}-\sum_{i=1}^{3}\frac{u_iu_i}{\omega^2}, \tag{15}$$

where the left sum is over the lattice phonons and the right sum is over the interstitial coordinates.

The interstitial is coupled to its environment through the perturbation (interaction) matrix Γ. From (4),

$$\Gamma_{ij}=(M_iM_j)^{-1/2}\Delta v_{ij}. \tag{16}$$

Application of the theory is then a straightforward procedure.

III. SYMMETRY PROPERTIES

The interstitial is assumed to occupy the $(\frac{1}{2},\frac{1}{2},\frac{1}{2})$ position in the unit cell of the diamond lattice. Calculations by Weiser[20] indicate that small charged interstitials may prefer the position $(\frac{5}{8},\frac{5}{8},\frac{5}{8})$. This latter position will not be considered, though the general conclusions of this paper should apply.

The symmetry of the environment of the interstitial is T_d. The nearest neighbors lie at the vertices of a regular tetrahedron while the next nearest neighbors are at the vertices of a regular octahedron. The axes of the octahedron pass through the edges of the tetrahedron maintaining the tetrahedral symmetry. Any Jahn-Teller distortion of the local environment should be small because of the small interaction of the interstitial with the lattice as compared with the interactions of the lattice atoms among themselves. This is indicated by the comparison of the energy of migration for an interstitial atom with the energy of creation of a vacancy-interstitial pair which are $\lesssim$0.5 and $\sim$5–6 eV, respectively.[17,21] A further indication is the small length change introduced into the Si or Ge lattice through radiation damage, though this latter could be accounted for by positive and negative volume changes for interstitial and vacancy.[22] The calculations that follow will ignore any change in the local symmetry which might arise through distortion.

A. The Symmetry Coordinates

The Cartesian coordinate system describing the interstitial and its local environment is chosen with the

[20] K. Weiser, Phys. Rev. **126**, 1427 (1962).

[21] G. D. Watkins, Bull. Am. Phys. Soc. **9**, 48 (1964); *Proceedings of the International Conference on the Physics of Semiconductors* (Dunod Cie., Paris, 1965); Vol. 3, p. 97.

[22] F. L. Vook, Phys. Rev. **125**, 855 (1962).

interstitial at the origin and axes passing through the vertices of the octahedron of next nearest neighbors. The tetrahedron of nearest neighbors is oriented with one vertex lying in the $(\bar{1},\bar{1},\bar{1})$ direction from the interstitial. The location and numbering of the atoms is given in Table I.

The symmetry coordinates have been obtained for the tetrahedron plus interstitial and the octahedron plus interstitial separately by the projection method.[23] The resultant coordinates are then orthogonalized where necessary. The set of coordinates spans the representation Γ_c of the group T_d given by

$$\Gamma_c = 2\Gamma_1 + 2\Gamma_{12} + 6\Gamma_{15} + 3\Gamma_{25}. \quad (17)$$

The coordinates are listed in Table II. The notation for the irreducible representations of T_d is that of Bethe.[24]

The matrices g, t, and γ must form Γ_1 representations of the group. From (17) it is noted that diagonalization of two 2×2, one 3×3, and one 6×6 matrix completes the diagonalization of the 33×33 $g\gamma$ matrix.

TABLE I. Location of atoms interacting with the interstitial. a = lattice constant; $r_m = \frac{1}{2}a$; $r_n = \frac{1}{4}a$.

Atom number	Location	Atom number	Location
1 (Interstitial)	(0,0,0)	7	$r_m(0,\bar{1},0)$
2	$r_n(\bar{1},\bar{1},1)$	8	$r_m(0,0,\bar{1})$
3	$r_n(1,\bar{1},1)$	9	$r_m(1,0,0)$
4	$r_n(1,1,\bar{1})$	10	$r_m(0,1,0)$
5	$r_n(\bar{1},\bar{1},\bar{1})$	11	$r_m(0,0,1)$
6	$r_m(\bar{1},0,0)$		

TABLE II. Symmetry coordinates of the complex of interstitial, nearest and next-nearest neighbors.

Γ_1 Representations

$(a,1) = (1/\sqrt{6})\{(x_6-x_9)+(y_7-y_{10})+(z_8-z_{11})\}$

$(a,2) = (1/\sqrt{12})\{(x_5+y_5+z_5)+(x_2-y_2-z_2)-(x_3-y_3+z_3)-(x_4+y_4-z_4)\}$

Γ_{12} Representations

$(e,1) = (1/\sqrt{12})\{(x_6-x_9)+(y_7-y_{10})-2(z_8-z_{11})\}$

$(e,2) = (1/\sqrt{24})\{(x_5+y_5-2z_5)+(x_2-y_2+2z_2)-(x_3-y_3-2z_3)-(x_4+y_4+2z_4)\}$

$(\theta,1) = (1/2)\{(y_7-y_{10})-(x_6-x_9)\}$

$(\theta,2) = (1/\sqrt{8})\{(y_5-x_5)-(y_2+x_2)+(y_3+x_3)-(y_4-x_4)\}$

Γ_{25} Representations

$(\xi,1) = (1/2)(x_8+x_{11}-x_{10}-x_7)$

$(\xi,2) = (1/2)(z_{10}-z_7+y_8-y_{11})$

$(\xi,3) = (1/\sqrt{8})(z_2+z_4-z_5-z_3+y_4+y_5-y_3-y_2)$

$(\eta,1) = (1/2)(y_6+y_9-y_{11}-y_8)$

$(\eta,2) = (1/2)(x_{11}-x_8+z_6-z_9)$

$(\eta,3) = (1/\sqrt{8})(y_4+y_3-y_5-y_2+x_3+x_5-x_2-x_4)$

$(\zeta,1) = (1/2)(z_7+z_{10}-z_9-z_6)$

$(\zeta,2) = (1/2)(y_9-y_6+x_7-x_{10})$

$(\zeta,3) = (1/\sqrt{8})(x_3+x_2-x_5-x_4+z_2+z_5-z_4-z_3)$

Γ_{15} Representations

$(x,1) = (1/\sqrt{6})(x_6+x_9-2x_1)$

$(x,2) = (1/(84)^{1/2})\{3(x_7+x_{10}+x_8+x_{11})-4(x_1+x_6+x_9)\}$

$(x,3) = (1/(308)^{1/2})\{7(x_2+x_3+x_4+x_5)-4(x_1+x_6+x_7+x_8+x_9+x_{10}+x_{11})\}$

$(x,4) = (1/(11)^{1/2})(x_1+x_2+x_3+x_4+x_5+x_6+x_7+x_8+x_9+x_{10}+x_{11})$

$(x,5) = (1/2)(y_{11}-y_8+z_7-z_{10})$

$(x,6) = (1/\sqrt{8})(z_2-z_5+z_4-z_3-y_4-y_5+y_3+y_2)$

$(y,1) = (1/\sqrt{6})(y_7+y_{10}-2y_1)$

$(y,2) = (1/(84)^{1/2})\{3(y_{11}+y_8+y_9+y_6)-4(y_1+y_7+y_{10})\}$

$(y,3) = (1/(308)^{1/2})\{7(y_2+y_3+y_4+y_5)-4(y_1+y_6+y_7+y_8+y_9+y_{10}+y_{11})\}$

$(y,4) = (1/(11)^{1/2})\{(y_1+y_2+y_3+y_4+y_5+y_6+y_7+y_8+y_9+y_{10}+y_{11})\}$

$(y,5) = (1/2)(x_8-x_{11}+z_9-z_6)$

$(y,6) = (1/\sqrt{8})(x_3-x_5+x_2-x_4-z_2-z_5+z_4+z_3)$

$(z,1) = (1/\sqrt{6})(z_8+z_{11}-2z_1)$

$(z,2) = (1/(84)^{1/2})\{3(z_6+z_9+z_7+z_{10})-4(z_1+z_8+z_{11})\}$

$(z,3) = (1/(308)^{1/2})\{7(z_2+z_3+z_4+z_5)-4(z_1+z_6+z_7+z_8+z_9+z_{10}+z_{11})\}$

$(z,4) = (1/(11)^{1/2})\{(z_1+z_2+z_3+z_4+z_5+z_6+z_7+z_8+z_9+z_{10}+z_{11})\}$

$(z,5) = (1/2)(y_6-y_9+x_{10}-x_7)$

$(z,6) = (1/8)(y_4-y_5+y_3-y_2-x_3-x_5+x_2+x_4)$

[23] J. S. Griffith, *The Theory of Transition Metal Ions* (Cambridge University Press, Cambridge, England, 1961), p. 167.
[24] H. Bethe, Ann. Physik 3, 133 (1929).

B. The Green's-Function Matrix

The interstitial contribution to the Green's-function matrix is evaluated from (15). The last sum contains the interstitial contribution. The three-by-three submatrix which gives the projection of g onto the subspace of the interstitial coordinates is given by

$$G(\text{int})=\begin{bmatrix}-1/\omega^2 & 0 & 0\\ 0 & -1/\omega^2 & 0\\ 0 & 0 & -1/\omega^2\end{bmatrix}. \tag{18}$$

All G_{ij} for which one of i, j refers to the interstitial and the other refers to an atom of the perfect lattice are zero. G_{ij} for both atoms in the perfect lattice is given by

$$G_{ij}(\omega^2)=\frac{n}{N}\sum_{kp}\frac{e_{kp}{}^i e_{kp}{}^{j*}e^{i\mathbf{k}\cdot\mathbf{r}}}{\omega_{kp}{}^2-\omega^2}, \tag{19}$$

where $\mathbf{r}$ is the vector from the atom represented by j to the atom represented by i. The star represents complex conjugation. The factor n, the number of atoms per primitive unit cell, is included so that the polarization vectors e_{kp} are normalized in a primitive unit cell. That is,

$$\begin{aligned}&\textstyle\sum_i e_{kp}{}^i e_{kp'}{}^{i*}=\delta_{pp'}, \text{ (primitive cell)}\\ &\textstyle\sum_p e_{kp}{}^i e_{kp}{}^{j*}=\delta_{ij}.\end{aligned} \tag{20}$$

The $e_{kp}{}^i$ form a basis for the primitive unit cell and are the same in each primitive unit cell.

From Eq. (17) it is determined that the matrices g and $g\gamma$ will have only 33 independent terms of the form (19) since they must be invariant under the symmetry group. It is thus necessary to evaluate only 33 terms of the form (19) in order to evaluate these matrices. In the numerical work the phonon spectrum is taken as spherically symmetric with transverse and longitudinal polarization. This increase in symmetry reduces the number of independent components to 20. This can be seen by expanding the exponential in (19) in a series of spherical harmonics as

$$G_{ij}(\omega^2)=\frac{4\pi n}{N}\sum_{lm}(i)^l \mathcal{Y}_l{}^{m*}(\theta_r,\varphi_r)\times\sum_{kp}\frac{e_{kp}{}^i e_{kp}{}^{j*}\mathcal{Y}_l{}^m(\theta_k,\varphi_k)j_l(kr)}{\omega_{pk}{}^2-\omega^2}, \tag{21}$$

where (θ_r,φ_r) are the angles describing the vector $\mathbf{r}$ while (θ_k,φ_k) are the corresponding angles for $\mathbf{k}$. The spherical Bessel function of order l is represented by $j_l(kr)$. The magnitudes of $\mathbf{k}$ and $\mathbf{r}$ are k and r, respectively.

The polarization vectors, which depend only on the atomic locations in the unit cell and not the absolute atomic positions in the lattice, form a three-dimensional ($l=1$) representation of the full rotation group. Since the second sum in (18) must be an identity representation of this group (in the approximation in which the numerical work is carried out) terms beyond $l=2$ must be zero. Thus (21) is truncated after the terms in $l=2$. The 3×3 part of g representing the matrix components between two atoms in the lattice can then be written as

$$\begin{aligned}
G_{xx}&=A(r)+[(2x^2-y^2-z^2)/r^2]E(r),\\
G_{yy}&=A(r)+[(2y^2-x^2-z^2)/r^2]E(r),\\
G_{zz}&=A(r)+[(2z^2-x^2-y^2)/r^2]E(r),\\
G_{xy}&=-(z/r)S(r)-3(xy/r^2)T(r),\\
G_{yx}&=(z/r)S(r)-3(xy/r^2)T(r),\\
G_{xz}&=(y/r)S(r)-3(xz/r^2)T(r),\\
G_{zx}&=-(y/r)S(r)-3(xz/r^2)T(r),\\
G_{yz}&=-(x/r)S(r)-3(yz/r^2)T(r),\\
G_{zy}&=(x/r)S(r)-3(yz/r^2)T(r),
\end{aligned} \tag{22}$$

where

$$\begin{aligned}
A(r)&=\frac{n}{N}(4\pi)^{1/2}\sum_{kp}\frac{e_{kp}{}^{x1}e_{kp}{}^{x2*}j_0(kr)\mathcal{Y}_0{}^0(\theta_k,\varphi_k)}{\omega_{pk}{}^2-\omega^2},\\
E(r)&=-\frac{n}{N}\left(\frac{40\pi}{3}\right)^{1/2}\sum_{kp}\frac{e_{kp}{}^{x1}e_{kp}{}^{x2*}j_2(kr)\mathcal{Y}_2{}^2(\theta_k,\varphi_k)}{\omega_{kp}{}^2-\omega^2},\\
S(r)&=\frac{n}{N}(24\pi)^{1/2}\sum_{kp}\frac{e_{kp}{}^{x1}e_{kp}{}^{z2*}j_1(kr)\mathcal{Y}_1{}^1(\theta_k,\varphi_k)}{\omega_{kp}{}^2-\omega^2},\\
T(r)&=-\frac{n}{N}\left(\frac{40\pi}{3}\right)^{1/2}\sum_{kp}\frac{e_{kp}{}^{x1}e_{kp}{}^{z2*}j_2(kr)\mathcal{Y}_2{}^1(\theta_k,\varphi_k)}{\omega_{kp}{}^2-\omega^2},\\
\mathbf{r}&=(x,y,z)=\mathbf{r}_1-\mathbf{r}_2
\end{aligned} \tag{23}$$

and $\mathbf{r}_1,\mathbf{r}_2$ are the position vectors of the two atoms.

The expressions (22) and (23) have been obtained by the use of the correct symmetry properties of the lattice and therefore are correct expressions for g through terms in $l=2$ in (21). In the limit of spherical symmetry in the phonon spectrum and transverse and longitudinal polarization the expressions are correct to all orders of the expansion (21).

The expressions (22) and (23) are no easier to evaluate than the expressions (19); however, use of Eqs. (22) and (23) reduces the bookkeeping necessary to evaluate the g matrix in the aforementioned approximation. The 20 expressions to be evaluated result from the five values of $\mathbf{r}$ for the four functions A, E, S, and T. For $\mathbf{r}=0$, the functions E, S, and T are zero, and if the two atoms occupy different positions in the diamond-lattice primitive unit cell, then S is zero. This reduces the number of expressions to 15 and a fortuitous geometrical factor eliminates the need for one of the E's reducing to 14 the number of independent expressions needed in evaluating g.

C. The Perturbation Matrix

The perturbation matrix includes the changes in force constants when the interstitial is allowed to couple the lattice. Coupling to the nearest and next nearest neighbors is assumed along with the assumption that the presence of the interstitial does not change the forces between the atoms of the lattice nor the symmetry of its local environment. The interaction potential is then given by

$$\begin{aligned} V_0 &= V_0(0)+a_{11}f_1(\mathbf{r}_i)+a_\perp f_2(\mathbf{r}_i)\,, \\ V_T &= V_T(0)+b_{11}f_3(\mathbf{r}_i)+b_\perp f_4(\mathbf{r}_i)\,, \end{aligned} \tag{24}$$

where

$$\begin{aligned} f_1(\mathbf{r}_i) &= (x_1-x_6)^2+(x_1-x_9)^2+(y_1-y_7)^2 \\ &\quad +(y_1-y_{10})^2+(z_1-z_8)^2+(z_1-z_{11})^2\,, \\ f_2(\mathbf{r}_i) &= \sum_{i=6}^{11}(\mathbf{r}_1-\mathbf{r}_i)^2-f_1(\mathbf{r}_i)\,, \\ f_3(\mathbf{r}_i) &= \tfrac{1}{3}(x_1-y_1-z_1-x_2+y_2+z_2)^2 \\ &\quad +(x_1-y_1+z_1-x_3+y_3-z_3)^2 \\ &\quad +(x_1+y_1-z_1+x_4-y_4+z_4)^2 \\ &\quad +(x_1+y_1+z_1-x_5-y_5-z_5)^2\,, \\ f_4 &= \sum_{i=2}^{5}(\mathbf{r}_1-\mathbf{r}_i)^2-f_3\,. \end{aligned} \tag{25}$$

In Eqs. (24) and (25) $\mathbf{r}_i$ represents the *displacement* of the ith atom from its equilibrium position. The numbering of atoms is as indicated in Table I. This form of the interaction is that required by the symmetry of the complex of atoms interacting with the interstitial in the harmonic approximation. V_0 is the interaction potential for the octahedron of next nearest neighbors while V_T is the interaction potential for the tetrahedron of nearest neighbors. Second derivatives of the above expressions then will yield the matrix ΔV_{ij} from which Γ_{ij} may be constructed.

Transformation of g and γ to the coordinate system of the symmetry coordinates can be carried out after some tedious algebra. The results are not presented here, but are used in the numerical calculations.

IV. NUMERICAL CALCULATIONS

A. The Green's-Function Matrix

The expressions (23) were evaluated using transverse- and longitudinal-polarized phonons. The spectrum was assumed to be spherically symmetric and a dispersion relation was used which agrees with the observed dispersion relation[1] in the (1,0,0) direction. The expressions were evaluated at frequencies of $n\omega_{LA}/40$, $n=1,2,\cdots,39$ (where ω_{LA} is the maximum frequency for the longitudinal-acoustic modes) and used in the evaluation of the g matrix.

B. The Interaction Matrix

The interaction matrix was taken as one of the independent variables in the calculation. Expressed in the symmetry coordinates, the interaction matrix depends on the following linear combinations of $a_\perp$, a_{11}, $b_\perp$, and b_{11}:

$$\begin{aligned} \alpha &= 2a_{11}\,, \\ \beta &= 2a_\perp\,, \\ \delta &= \tfrac{2}{3}(b_{11}+2b_\perp)\,. \end{aligned} \tag{26}$$

An estimate of the sizes of α, β, and δ can be obtained by noting that the migration energy of the interstitial is $\lesssim 0.5$ eV.[17,21] Holding the lattice atoms fixed and moving the interstitial half the distance from one interstitial position to the next should provide an approximate method of relating the migration energy to the coupling constants.

Using the expression (21) for the potential this method gives $K=(\alpha+2\beta+2\delta)=5.0$ kerg/cm² for a migration energy of 0.5 eV. For a slightly different model of the potential, namely $V=V_0\sum_i e^{-\mu|\mathbf{r}_1-\mathbf{r}_i|}$, adjusting the parameters V_0 and μ to give a migration energy of 0.5 eV and a maximum value for K, yields $K=4.0$ kerg/cm². Electrostatic interactions can give larger K values for a given migration energy. They must be attractive, however, and will reduce the force constant for an interstitial located at $(\frac{1}{2},\frac{1}{2},\frac{1}{2})$. Implicit in this analysis is the assumption that interstitial migration proceeds along the body diagonal rather than via a substitutional path.

In view of the above discussion the values of α, β, and δ were allowed to vary such that $0\leq K\leq 30.0$ kerg/cm². In addition to a variation of force constants the interstitial mass was varied from 0.05 times the host mass to 1.65 times the host mass in Ge and to 2.00 times the host mass in Si. The numerical calculations were carried

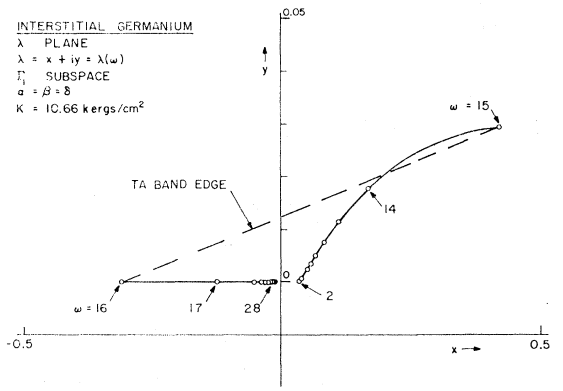

FIG. 1. Graphical representation of $\lambda(\omega)$, an eigenvalue of the $g\gamma$ matrix, in the Γ_1 subspace of the matrix. The resonance frequency ω is determined from $\mathrm{Re}\lambda(\omega)=-1$ (see Eq. 12); thus no resonances are indicated in this figure. The dashed line connects a frequency just below the transverse-acoustic band edge with one just above. The dashed line has no other significance. The frequency is given in units of $\omega_{LA}/40$, where ω_{LA} is the longitudinal-acoustic band-edge frequency in the (1,0,0) direction.

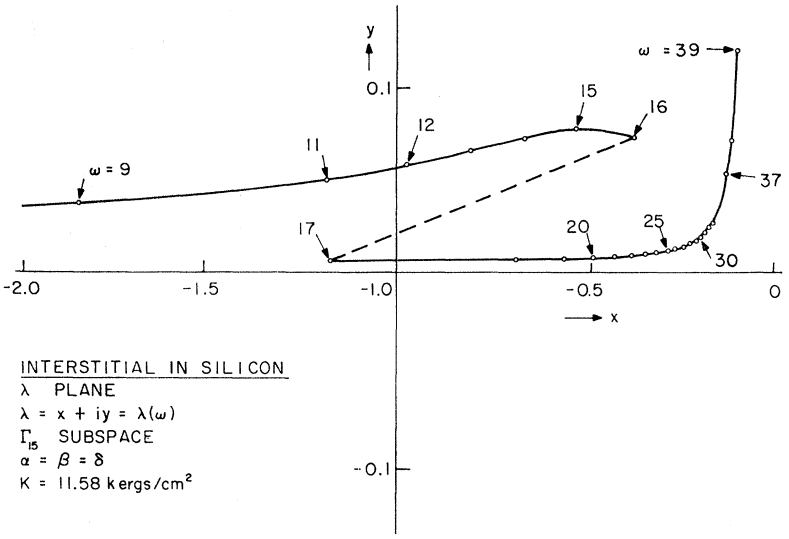

FIG. 2. Graphical representation of $\lambda(\omega)$, an eigenvalue of the $g\gamma$ matrix in the Γ_{15} subspace of the matrix. The resonance frequency ω is determined from $\mathrm{Re}\lambda(\omega)=-1$ (see Eq. 12); thus two resonances are indicated in this figure at frequencies $\sim$11.9 and $\sim$17.3. The dashed line indicates the transition across the transverse-acoustic (TA) band edge, but its location is not significant. Frequency units are the same as in Fig. 1.

out on the CDC 1604 computer at the Sandia Corporation, Albuquerque, New Mexico.

V. RESULTS

A. Resonant Frequency

Typical dependence of the $g\gamma$ eigenvalues on frequency is show in Figs. 1 and 2. The transverse-acoustic band edge occurs at $\omega=16.6$ for Si and at $\omega=15.4$ for Ge. The dashed lines on the figures thus connect frequencies just below this band edge with those just above it. The model of the phonon field used is most in error in this region, and detailed comments on the behavior of the eigenvalues across the band edge are not justified. This region is ignored then; note that resonances occurring near the band edge will be difficult to resolve from other band-edge effects.

The eigenvalues are proportional to K for fixed ratios of the force constants α, β, and δ. It is then possible to contract or expand the eigenvalues about the origin by changing the force constants. For appropriate values of K the eigenvalues having the frequency dependence of Fig. 1 can lead to resonances satisfying the condition (12). These resonances will occur only above the transverse-acoustic band edge and require in all cases $K\geq 30$ kerg/cm². In view of the discussion on the expected magnitude of K it is unlikely that eigenvalues of this form will produce resonances.

The eigenvalues of the form shown in Fig. 2 will always produce at least one resonance for $K\leq 30$ kerg/cm² and can produce two. When a single resonance is produced it lies inside the transverse-acoustic band, and when there are two, one lies within the transverse-acoustic band and one lies above it. The resonance lying above the transverse-acoustic band occurs only for $K\geq 10$ kerg/cm² and has been investigated only for interstitial mass equal to host mass.

Three of the eigenvalues of the Γ_{15} block of the $g\gamma$ matrix have the form shown in Fig. 2, and all remaining eigenvalues of $g\gamma$ are of the form shown in Fig. 1. The three eigenvalues leading to resonances are degenerate, and thus a single resonance will be associated with the interstitial in Ge or in Si.

The resonance frequency is shown as a function of K

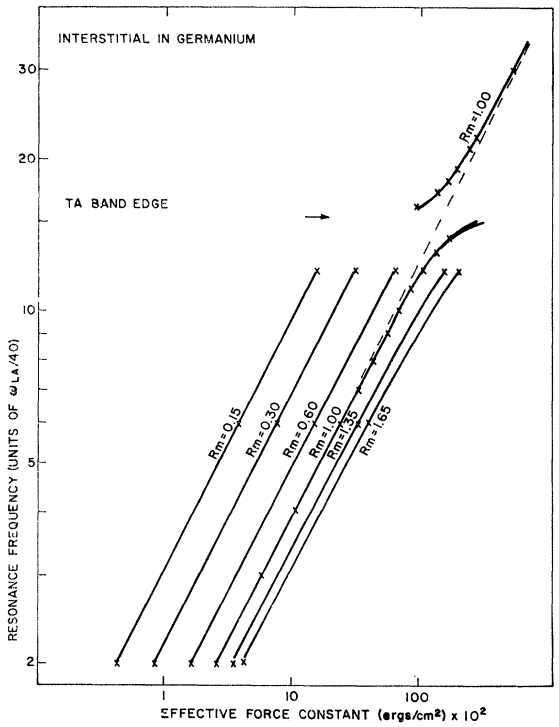

FIG. 3. Resonance frequency ω versus effective force constant $K=(\alpha+2\beta+2\delta)$ for interstitial atoms in germanium. The dashed line indicates $\omega\propto K^{1/2}$. R_m is the ratio of interstitial atom mass to germanium atom mass. Curves are all for $\alpha=\beta=\delta$, except that the branching of the $R_m=1.00$ curve just below the TA band edge indicates the effect of using $2\alpha=2\beta=\delta$. The lower branch corresponds to the latter choice.

TABLE III. Comparison of effective force constants for various ratios of α, β, and δ. Transverse-acoustic band edge is at $\omega=15.4$ in germanium and $\omega=16.6$ in silicon.

	Germanium					Silicon				
ω	1	2	3	4	5	1	2	3	4	5
2.0	2.52	2.52	2.52	2.52	2.52	2.95	2.95	2.95	2.95	2.95
4.0	10.2	10.2	10.2	10.2	10.2	11.9	11.9	11.9	11.9	11.9
6.0	23.2	23.2	23.2	23.2	23.2	27.0	27.0	27.1	27.0	27.0
8.0	42.2	42.4	42.3	42.0	42.1	49.0	48.9	49.4	48.9	49.0
10.0	68.5	69.1	68.8	67.9	68.2	···	78.5	80.1	78.5	78.9
12.0	105.5	···	106.3	103.5	104.6	119.4	118.1	123.2	118.0	119.3
15.0	268.3	···	301.4	224.6	247.1	225.3	215.2	268.2	214.0	···

Germanium	Silicon
1 $\alpha=\beta=\delta$	1 $\alpha=\beta=\delta$
2 $\alpha=2\beta=\delta$	2 $\alpha=\beta=10\delta$
3 $2\alpha=2\beta=\delta$	3 $\alpha=10\beta=\delta$
4 $2\alpha=\beta=2\delta$	4 $10\alpha=\beta=\delta$
5 $2\alpha=\beta=\delta$	5 $10\alpha=2\beta=\delta$

in Fig. 3 for Ge and Fig. 4 for Si. The parameter varying from one curve to another in the figures is R_m, the ratio of the interstitial mass to the host mass. Except near the transverse-acoustic band edge the resonance frequency varies nearly as $K^{1/2}$. For a fixed frequency it is also noted that the ratio K/R_m is nearly constant varying by about $\pm 5\%$ over the range of values of R_m. Thus $\omega \propto (K/M)^{1/2}$ except near the transverse-acoustic band edge, the expression becoming more accurate as we move away from the band edge.

For a given value of K and R_m the resonance frequency is relatively insensitive to the individual values of α, β, and δ except near the transverse-acoustic band edge. This is indicated in Table III for both Ge and Si.

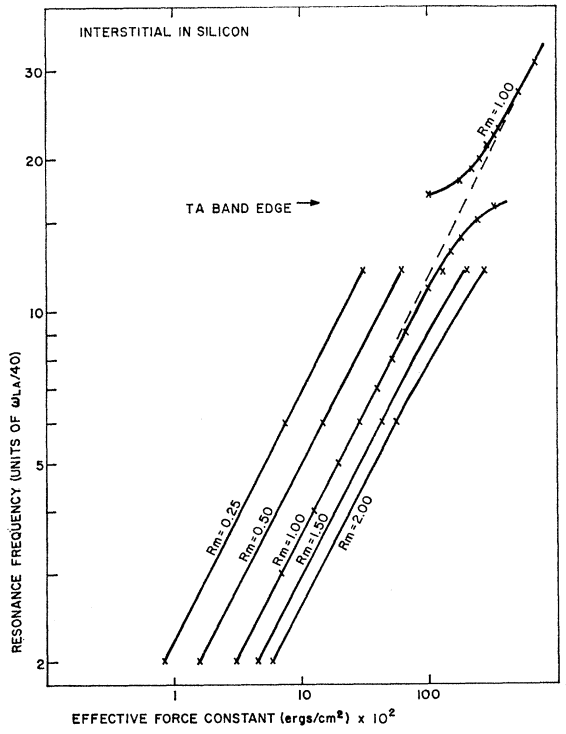

FIG. 4. Resonance frequency ω versus effective force constant $K=(\alpha+2\beta+2\delta)$ for an interstitial atom in silicon. The dashed line indicates $\omega \propto K^{1/2}$. Curves are all for $\alpha=\beta=\delta$.

In the initial calculations if the lattice contribution to the Green's-function matrix had been set equal to zero, the results indicated above as approximate would have been exact. It is thus concluded that the lattice contributes very little to the location of an interstitial-associated acoustic phonon resonance except when the resonance falls near the transverse-acoustic band edge. The lattice is thus very stiff and the interstitial may be effectively considered for most values of the force constant to be a simple mass on a spring.

B. The Resonance Width

The dependence of the $g\gamma$ eigenvalue on frequency as shown in Fig. 2 can be represented in the acoustic band by

$$\begin{aligned} &\mathrm{Re}\lambda = c(\omega)/\omega^2, \\ &\mathrm{Im}\lambda \approx \mathrm{const}\times\omega, \end{aligned} \tag{27}$$

where $c(\omega)$ is a slowly varying function of ω. Placing this functional dependence into the expression for the resonance width (13) yields

$$\Delta\omega \approx \omega|\mathrm{Im}\lambda| = \omega y. \tag{28}$$

The quantity $y \approx \Delta\omega/\omega$ is plotted in Fig. 5 for Ge and Fig. 6 for Si as a function of resonance frequency. As in Figs. 3 and 4, the variable characterizing the various curves is the interstitial mass R_m.

The set of curves in Figs. 5 and 6 can be approximately represented by the formula $y \propto \omega^n M^k$ with $n \cong 3$ and $k \cong 1$. The curves show that a measurement of both ω and y would allow a determination of R_m (or M) from which Figs. 3 or 4 would yield K.

C. The Resonance Eigenvectors

Typical behavior of the resonance eigenvectors as functions of resonance frequency, force-constant ratios,

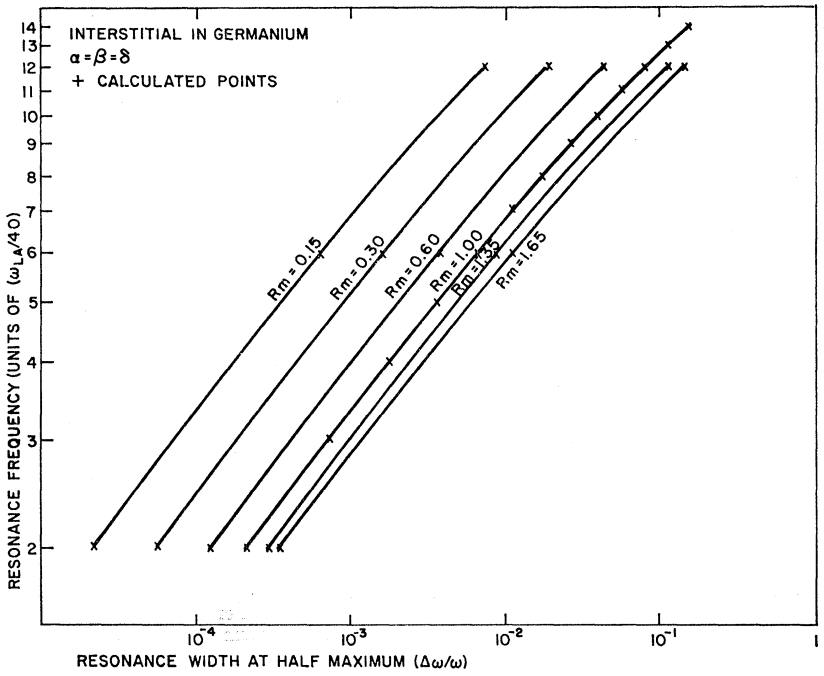

FIG. 5. Resonance frequency ω versus resonance width at half-maximum for interstitial atom in germanium. R_m is the ratio of interstitial-atom mass to germanium-atom mass.

and mass ratio is shown in Tables IV, V, and VI, respectively. The coupling of phonons into the resonance will depend on the left eigenvectors η_s, while the coupling out of the resonance will depend on the right eigenvectors ξ_s as discussed at the end of Sec. IIA.

The eigenvectors presented in the tables all involve the x components of the various atoms involved in the resonance. The two other resonances, degenerate with the resonance indicated, will involve similar eigenvectors with respect to the y and z displacements. These eigenvectors may be obtained from those in the tables by an appropriate rotation of the coordinate system.

The complete eigenvectors are not presented in the tables. The displacements of the remaining atoms may

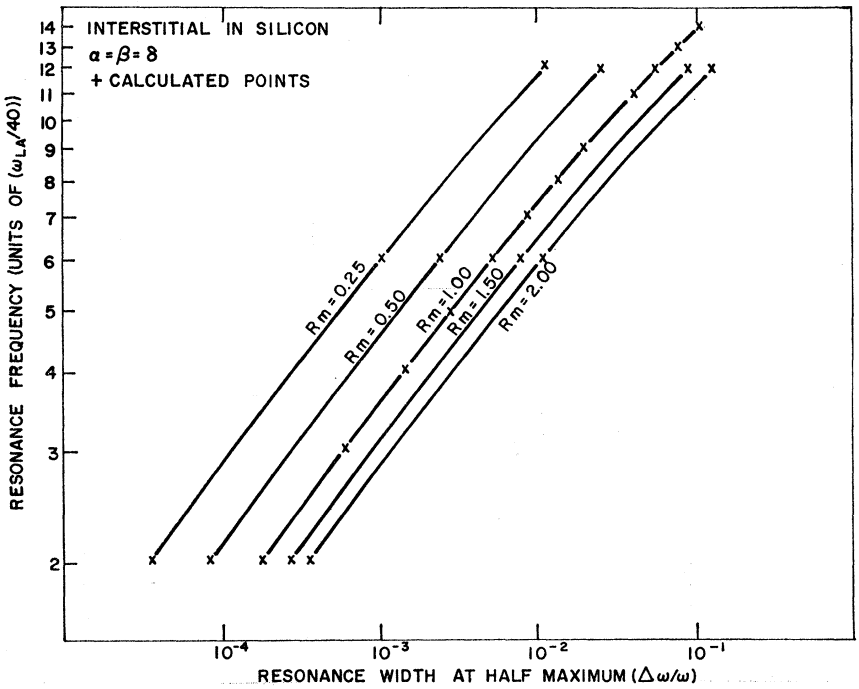

FIG. 6. Resonance frequency ω versus resonance width at half-maximum for interstitial atom in silicon. R_m is the ratio of interstitial-atom mass to silicon-atom mass.

TABLE IV. Resonance eigenvectors as a function of frequency (germanium). $R_m=1.00$; $2\alpha=2\beta=\delta$. The correct coefficients for the right eigenvectors are obtained by adding $i\times$Imaginary to each of x_1, $x_2,\cdots$, etc. The left-eigenvector coefficients are correct as presented. The coefficients for the other x_i may be obtained from those given through the relations $x_2=x_3=x_4=x_5$, $x_6=x_9$, and $x_7=x_8=x_{10}=x_{11}$.

Right eigenvectors ω	2.00	4.00	6.00	8.00	10.00	12.00
x_1	1.0000	0.9994	0.9966	0.9870	0.9600	0.9027
x_2	0.0029	0.0116	0.0268	0.0502	0.0844	0.1323
x_7	0.0023	0.0095	0.0218	0.0397	0.0643	0.0895
x_6	0.0030	0.0125	0.0294	0.0556	0.0954	0.1537
Imaginary	0.0002	0.0018	0.0065	0.0170	0.0370	0.0700

Left eigenvectors ω	x_1	x_2	x_7	x_6
2.00	1.029	−0.1432	−0.0716	−0.0716
4.00	1.012	−0.1445	−0.0724	−0.0722
6.00	1.030	−0.1469	−0.0739	−0.0733
8.00	1.065	−0.1518	−0.0767	−0.0754
10.00	1.137	−0.1616	−0.0827	−0.0798
12.00	1.302	−0.1842	−0.0968	−0.0894

TABLE V. Resonance eigenvector dependence on the ratios of α, β, and δ (germanium). $\omega=6.00$, $R_m=1.00$. The correct coefficients for the right eigenvectors are obtained by adding $i\times$Imaginary to each of the x_1, $x_2,\cdots$, etc. The left-eigenvector coefficients are correct as presented. The coefficients for the other x_i may be obtained from those given through the relations $x_2=x_3=x_4=x_5$, $x_6=x_9$, and $x_7=x_8=x_{10}=x_{11}$.

Right eigenvectors	1	2	3	4	5
x_1	0.9966	0.9964	0.9966	0.9969	0.9967
x_2	0.0264	0.0273	0.0268	0.0253	0.0259
x_6	0.0289	0.0302	0.0294	0.0274	0.0290
x_7	0.0215	0.0220	0.0218	0.0209	0.0222
Imaginary	0.0065	0.0065	0.0065	0.0065	0.0065

Left eigenvectors	x_1	x_2	x_6	x_7	
1	1.029	−0.1027	−0.1025	−0.1033	1 $\alpha=\beta=\delta$
2	1.031	−0.1288	−0.1284	−0.0684	2 $\alpha=2\beta=\delta$
3	1.030	−0.1470	−0.0733	−0.0739	3 $2\alpha=2\beta=\delta$
4	1.027	−0.0732	−0.0730	−0.1470	4 $2\alpha=\beta=2\delta$
5	1.028	−0.1140	−0.0569	−0.1146	5 $2\alpha=\beta=\delta$

TABLE VI. Resonance eigenvectors as a function of interstitial mass (germanium). $\omega=6.00$, $\alpha=\beta=\delta$. The expressions for the x_i under the right-eigenvector heading, (a,b), imply that the coefficient of x_i is the complex number $a+ib$. The imaginary part of the left eigenvectors is too small to be included in the table. The coefficients for the x_i not listed may be obtained from the relations $x_2=x_3=x_4=x_5$, $x_6=x_9$, and $x_7=x_8=x_{10}=x_{11}$.

Right eigenvectors R_m	0.20	0.50	0.75	1.00	1.35	1.65
x_1	(0.9991, 0.0009)	(1.003, 0.0030)	(0.9970, 0.0048)	(0.9966, 0.0065)	(0.9954, 0.0089)	(0.9984, 0.0108)
x_2	(0.0104, 0.0022)	(0.0187, 0.0045)	(0.0230, 0.0056)	(0.0268, 0.0065)	(0.0306, 0.0076)	(0.0336, 0.0085)
x_6	(0.0119, 0.0025)	(0.0185, 0.0045)	(0.0253, 0.0057)	(0.0294, 0.0065)	(0.0336, 0.0078)	(0.0353, 0.0086)
x_7	(0.0083, 0.0025)	(0.0150, 0.0044)	(0.0187, 0.0055)	(0.0218, 0.0065)	(0.0250, 0.0077)	(0.0271, 0.0083)

Left eigenvectors R_m	x_1	x_2	x_6	x_7
0.20	1.005	−0.0497	−0.0757	−0.0102
0.50	1.014	−0.0765	−0.0929	−0.0515
0.75	1.022	−0.0923	−0.1032	−0.0758
1.00	1.030	−0.1055	−0.1118	−0.0960
1.35	1.040	−0.1212	−0.1220	−0.1201
1.65	1.048	−0.1329	−0.1296	−0.1382

be obtained from those presented through the relations

$$x_2=x_3=x_4=x_5,$$
$$x_6=x_9, \tag{29}$$
$$x_7=x_8=x_{10}=x_{11}.$$

Note that phonons involve only displacements of the atoms 2 to 11 and will therefore couple either in or out of the resonance only through these coordinates. External radiations (gamma rays, neutrons, etc.) may, however, couple in or out through the interstitial coordinates (x_1,y_1,z_1).

Table IV shows that the coupling into the resonance is relatively insensitive to the resonance frequency, while the coupling out is a monotonically increasing function of resonance frequency for frequencies within the lowest acoustic band. For broad resonances the monotonic increase of coupling with frequency will lead to a small shift of the resonant frequency to higher frequencies, and a similar change will occur in the resonance width. These shifts are negligible, being of the order of a few percent near the band edge.

Table V shows the eigenvector dependence on the ratios of α, β, and δ. The coupling out of the resonance is seen to be relatively insensitive to changes in the ratios of the force constants, while the coupling in depends quite strongly on the force-constant ratios. Some insight into the this difference between the parts of the resonance-scattering event is gained by noticing the relative phase between the interstitial motion and the lattice motion as indicated in Tables IV, V, and VI. The excitation of the resonance occurs when the lattice and the interstitial are moving out of phase while the de-excitation of the resonance occurs during in-phase motion. It is clear then that the force constants would play an important role in the out-of-phase excitation, but would have relatively little effect on the in-phase de-excitation. The small effect that the force constants do have on the right eigenvectors (which determine the de-excitation) is due to the slightly out-of-phase motion of the lattice and interstitial.

The mass dependence of the eigenvectors is contained in Table VI. Entries in this table show that the coupling of the resonance to both incoming and outgoing phonons increases with increasing mass. This is in accord with intuition. The entries in Tables IV, V, and VI apply to the Ge lattice. Similar results are obtained for the Si lattice, but are not presented here.

VI. DISCUSSION

In the previous sections it has been shown that interstitial atoms in the $(\frac{1}{2},\frac{1}{2},\frac{1}{2})$ site in silicon and germanium are expected to resonantly scatter acoustic phonons. For reasonable choices of the interstitial-lattice forces a single resonant frequency results which is related to the forces through an effective force constant K. In addition, the frequency varies as the inverse square root of the interstitial mass, as expected. The resonance width also depends on the effective force constant and interstitial mass. A measurement of both the resonance frequency and width will thus allow an unambiguous determination of the effective force constant and the interstitial mass.[25]

In the process of determining the resonance frequencies, the resonance eigenvectors and eigenvalues of the $g\gamma$ matrix have also been calculated. These eigenvectors and eigenvalues can be used to construct the scattering matrix at the resonance frequency. Because of the simple model of the phonon field used in these calculations, the calculated eigenvectors may only be approximate. Before more complicated models of the phonon field are considered, however, there should be some comparison of the present calculations with experiment. No observations of interstitial atoms located in the $(\frac{1}{2},\frac{1}{2},\frac{1}{2})$ site of the unit cell have been reported for silicon or germanium.[26] A few methods are thus suggested by which observations might be made.

A. Proposed Methods of Observation

The proposed methods of observing the interstitial resonance, which will be briefly discussed here, include spin-lattice relaxation effects, infrared absorption, phonon-assisted electronic transitions, and low-temperature thermal conductivity. Mössbauer observation of similar resonances has previously been discussed in the literature,[12] and the general conclusions should apply to observation of the interstitial resonance. Infrared absorption measurements of similar resonances have also been recently reported[27] as have theoretical and experimental discussions of effects on low-temperature thermal conductivity.[15,28]

1. Spin-Lattice Relaxation

Spin-lattice relaxation which proceeds through local modes has been detected for hydrogen in CaF_2.[29] Similar results should be obtained for spin systems in the vicinity of an interstitial, with relaxation proceeding through phonons having the resonance frequency. The presence of the interstitial resonant-scattering center causes the density of phonon states in the vicinity of the interstitial at the resonant frequency to be increased over the density of states at other frequencies; this should lead to an exponential temperature de-

[25] Similar results would be expected for the interstitial bound in the $(\frac{5}{8},\frac{5}{8},\frac{5}{8})$ position in the unit cell, with two resonant frequencies instead of one because of the reduced symmetry in this site.

[26] As this paper was in its final draft a paramagnetic center in neutron-irradiated silicon was tentatively identified as an interstitial silicon ion. [I. Chen and C. Kikuchi, Bull. Am. Phys. Soc. **10**, 582 (1965).] Though the authors do not identify the location of this center in the unit cell they report an isotropic g factor, consistent with the T_d symmetry of the $(\frac{1}{2},\frac{1}{2},\frac{1}{2})$ site.

[27] A. J. Sievers, Phys. Rev. Letters **13**, 310 (1964).

[28] C. T. Walker and R. O. Pohl, Phys. Rev. **131**, 1433 (1963).

[29] D. W. Feldman, J. G. Castle, Jr., and J. Murphy, Bull. Am. Phys. Soc. **9**, 740 (1964).

pendence in the Raman relaxation time of the spin system. The relaxation through the quasilocal modes should be more easily observable than the relaxation through local modes since the energy is more nearly conserved in the intermediate states for the quasilocal-mode case. The exponential temperature dependence is similar to that predicted by Orbach when phonon scattering proceeds in resonance with an excited electronic state.[30]

2. *Infrared Absorption*

Charged interstitial atoms should exhibit infrared absorption with a peak absorption at (or near) the phonon-scattering resonance. That is, the resonance should be excited by absorption of the incident radiation, and it should decay through the lattice modes. The x_1 component of the eigenvectors presented in Tables IV, V, and VI will be important in this process.

For interstitial mass of the order of the host mass ($R_m \approx 1$) the expected location of such absorption would be in the range 0–100 cm^{-1} for Si and 0–50 cm^{-1} for Ge. These ranges are chosen on the basis of the earlier discussion of migration energy and are chosen such that $K \leq 10.0$ kerg/cm^2.

For interstitials which are weakly bound to the lattice the expected absorption would be in the lower portion of these frequency ranges and would be inaccessible through present infrared techniques. This might be the case for Si interstitials in Si which seem to be mobile at very low temperatures.[21] Similar behavior would be expected for the Ge interstitial in Ge. Impurity interstitials are more tightly bound, being mobile around 200°C,[21] and might be observable through infrared absorption measurements.

3. *Phonon-Assisted Electronic Transitions*

Absorption bands associated with electronic transitions in the vicinity of the interstitials should exhibit effects which are related to the presence of the interstitial. In particular these bands should be accompanied by peaks associated with 0, 1, 2, $\cdots$, etc., resonance phonons being created (or absorbed) simultaneously with the electronic transition. If the electronic states are very sharp and the interstitial resonance is isolated in frequency from other phonon modes which might be simultaneously created with the electronic transition, the one-phonon line associated with the resonant phonons should have very nearly the shape of the phonon-scattering resonance at low temperatures. A fairly accurate measurement of the resonance width might be possible through such effects, as well as the resonance frequency.

[30] R. Orbach, Proc. Phys. Soc. (London) **77**, 821 (1961).

4. *Low-Temperature Thermal Conductivity*

Low-temperature thermal-conductivity measurements should provide a complementary probe to the methods listed above. Wagner[15] has predicted minima in the thermal-conductivity curves associated with resonant scattering of phonons by substitutional defects. These minima have been observed by Walker and Pohl[28] and are quite broad. Similar results should be obtained for interstitial associated resonances.

If electrons are also associated with the interstitial, effects which concern both the electronic scattering resonances and the interstitial scattering resonances might be observed. In particular, interference between these two modes of phonon scatteting might lead to the narrow minima in the thermal-conductivity curves observed by Goff[31] and Vook.[32] Griffin and Carruthers[33] have previously tried to explain Goff's results on the basis of resonant scattering of the phonons through the electronic states alone. These calculations did not reproduce the observed minima.

5. *Mössbauer Absorption*

Mössbauer absorption should also give information concerning the interstitial. Mössbauer absorption associated with the resonant scattering of phonons by substitutional defects has been previously discussed in the literature[12] and the general conclusions of this discussion should apply to the present case.

VII. CONCLUSIONS

The calculations presented in this paper show that resonant scattering of phonons exists for reasonable choices of interstitial-lattice forces. Observation of these resonances would seem to be most probable through ESR experiments or phonon-assisted electronic transitions, though extension of infrared measurements to longer wavelengths might provide some interesting results. Low-temperature thermal conductivity measurements should corroborate measurements made by other means although it is thought that detailed identification of various defects would be difficult by this method.

ACKNOWLEDGMENTS

The author would like to thank F. L. Vook, G. W. Arnold, and J. A. Baldwin, Jr., for helpful discussions of the present problem. Also, thanks are due to D. C. Wallace and R. E. Nettleton for reading the manuscript before publication.

[31] J. F. Goff, Ph.D. thesis, Purdue University, 1962 (unpublished).
[32] F. L. Vook, Phys. Rev. **138**, A1234 (1965).
[33] A. Griffin and P. Carruthers, Phys. Rev. **131**, 1976 (1963).